PHYSICAL REVIEW B VOLUME 51, NUMBER 20 15 MAY 1995-II

Electron-electron interactions, coupled plasmon-phonon modes, and mobility in n-type GaAs

B.A. Sanborn
Semiconductor Electronics Division, National Institute of Standards and Technology, Gaithersburg, Maryland 20899
(Received 11 January 1995)

This paper investigates the mobility of electrons scattering from the coupled system of electrons and longitudinal-optical (LO) phonons in n-type GaAs. The Boltzmann equation is solved exactly for low electric fields by an iterative method, including electron-electron and electron–LO-phonon scattering dynamically screened in the random-phase approximation (RPA). The LO-phonon self-energy is treated in the plasmon-pole approximation. Scattering from ionized impurities screened in static RPA is calculated with phase-shift cross sections and scattering from RPA screened deformation potential and piezoelectric acoustic phonons is included in the elastic approximation. The results show that dynamic screening and plasmon-phonon coupling significantly modify inelastic scattering at low temperatures and densities. The effect on mobility is obscured by ionized impurity scattering in conventionally doped material, but should be important in modulation doped structures. For uncompensated bulk n-type GaAs, the RPA phase-shift model for electron-impurity scattering gives lower drift mobilities than the standard Thomas-Fermi or Born calculations, which are high compared to experiment. Electron-electron scattering lowers the mobility further, giving improved agreement with experiment, though discrepancies persist at high donor concentrations ($n > 10^{18}$ cm^{-3}). When impurities are ignored, inelastic scattering from the coupled electron-phonon system is the strongest scattering mechanism at 77 K for moderate doping. This result differs from the standard model, neglecting mode coupling and electron-electron scattering, which has the acoustic modes dominant in this regime.

I. INTRODUCTION

Good quantitative agreement between previous calculations and experiment on low-field transport coefficients of most high-purity polar semiconductors[1] suggests that the basic electron interactions are well understood in these materials. This is not the case for doped polar semiconductors. A long-standing discrepancy between theoretical and experimental mobility values for moderately to heavily doped n-type GaAs has been noted by many authors.[2–13] The fact that calculated mobilities are consistently too high, especially for moderate to heavy doping and low temperatures, has motivated suggestions that compensation effects,[7] correlated impurity distributions,[4,10] modifications of screening theory for a multi-ion system,[3] or multiple scattering from ionized impurities[13] should be included to obtain accurate results.

At the same time, it is known that electron-electron interactions can strongly influence electron transport in doped semiconductors, by screening matrix elements and renormalizing phonon energies, and through electron-electron scattering. More accurate treatments of electron-electron interactions frequently improve agreement between theory and experiment. For example, screening of ionized impurity potentials in the static random-phase approximation (RPA) rather than the commonly used linearized Thomas-Fermi approximation (LTFA) has been shown[14] to reduce theoretical electron mobility in n^+ silicon by more than a factor of 2 at 77 K. Including dynamically screened electron-electron scattering gives a significant reduction in drift velocity of hot electrons injected into n-type GaAs devices.[15] Calculations including the coupling between plasmons and longitudinal-optical (LO) phonons give shorter electron inelastic lifetimes[16,17] and enhanced hot-electron energy relaxation[18,19] in n-type GaAs. Previous attempts to include electron-electron scattering in GaAs mobility studies have been limited to static Thomas-Fermi screening of single-particle scattering.[8] So far, a treatment of inelastic scattering from the nonequilibrium coupled mode system in combination with an accurate model of ionized impurity scattering has not been attempted.

In Ref. 20, the inelastic collision term in the electron Boltzmann equation was derived by making the Born approximation and the RPA for scattering from the coupled electron–LO-phonon system in a doped polar semiconductor. The result is the sum of an electron-electron collision term and an electron–LO-phonon collision term that includes plasmon-phonon mode coupling. Both interactions are dynamically screened by only the electronic part of the total dielectric function for the electron-phonon system. The present paper describes an iterative method for exactly solving the low-field Boltzmann equation including the dynamically screened inelastic collision terms for arbitrary electron degeneracy and spherical energy surfaces.

For steady-state transport, electron-plasmon scattering is correctly accounted for by dynamically screening the electron-electron collision term.[20] Electron-plasmon

 ©1995 The American Physical Society

and electron-electron scattering events conserve total electron momentum and energy in direct gap doped semiconductors since umklapp processes are negligible in these materials. Therefore, the purely electronic scattering events cannot by themselves degrade an electrical curent, if spherical energy surfaces are assumed, and they merely rearrange the nonequilibrium electron momentum distribution produced by an applied field, thereby changing the probabilities for other scattering processes.

In the present work, the effect of electronic scattering is accounted for by solving the Boltzmann equation for the nonequilibrium electron distribution with electron-electron, electron-phonon, and electron-impurity scattering treated simultaneously. An isotropic effective electron mass and parabolic energy bands are assumed. The phonon distribution is approximated by its equilibrium form and the plasmon-pole approximation[21,22] is used in the LO phonon self-energy. Numerical results are presented for electron drift mobility in uncompensated n-type GaAs, including also electron scattering from piezoelectric and deformation potential acoustic phonons screened in the static RPA. The calculations for conventionally doped material include phase-shift scattering from ionized impurity potentials screened in the static RPA. This method gives lower mobilities than LTFA or Born calculations of electron-impurity scattering, in better agreement with experiment. Results for n-type GaAs with no impurities present show that electron-electron scattering and mode coupling rather dramatically alter inelastic scattering at 77 K, suggesting that these effects are significant for modulation doped material at low temperature.

This paper is organized as follows. Section II discusses the screening functions appropriate for the various electron scattering mechanisms included in this study. Section III describes the iterative method used to solve the Boltzmann equation. Section IV presents the numerical results with discussion emphasizing the differences obtained by using RPA vs LTFA screening and by including electron-electron scattering and plasmon–LO-phonon coupling.

II. SCREENING IN A MULTICOMPONENT SYSTEM

In Ref. 20, it was shown that the nonequilibrium character of screened electron interactions is essential to obtaining the correct form of the collision terms in the Boltzmann equation, which contain nonequilibrium distribution functions for the system's excitations. When this is done, there remain dielectric functions that screen the interaction matrix elements in the collision terms. When the Boltzmann equation is linearized with respect to electric field strength, only terms with equilibrium dielectric functions screening the matrix elements in the collision terms are nonvanishing. Therefore, consider the equilibrium screening process. The interaction between two test charges in a solid can be expressed as the bare Coulomb interaction $v_q = 4\pi e^2/q^2$ screened by the total dynamic dielectric function $\epsilon_T(q,\omega)$ for the system, including contributions from both the conduction and the lattice charges. The frequency dependence of the screened interaction is determined by the energy difference between the scattering electron's final and initial states.

In the RPA, the electron-electron interaction is equivalent to the test-charge–test-charge interaction. In the same approximation, the total interaction $v_q/\epsilon_T(q,\omega)$ is separable into a purely electron-electron interaction plus an electron-phonon interaction including a phonon self-energy term, each of these interactions being screened by only the electronic part of ϵ_T. The screened electron-phonon interaction $V_{\text{sc-ph}}$ includes the interactions with *all* relevant phonons. It can be determined[23] by subtracting from the total interaction the purely electronic interaction $v_q^\infty/\epsilon(q,\omega)$,

$$V_{\text{sc-ph}}(q,\omega) = \frac{v_q}{\epsilon_T} - \frac{v_q^\infty}{\epsilon} \tag{1}$$

$$= \frac{V_{\text{ph}}}{\epsilon[1-(v_q^\infty + V_{\text{ph}})P]}\,, \tag{2}$$

where $v_q^\infty = v_q/\epsilon_\infty$, $\epsilon(q,\omega) = 1 - v_q^\infty P(q,\omega)$ is the electronic RPA dielectric function, and P denotes the polarization of the noninteracting electron gas in this paper. The bare electron-phonon interaction V_{ph} is the sum over all phonon modes λ of the product of the phonon Green's function D_λ and the interaction matrix element M_λ squared $V_{\text{ph}} = \sum_\lambda |M_\lambda|^2 D_\lambda(q,\omega)$. This method was used in Ref. 20 in order to determine the screened electron–LO-phonon interaction $V_{\text{sc-LO}}$ for the case when only LO phonons are present ($V_{\text{ph}} = V_{\text{LO}}$).

When acoustic phonons are present as well, $V_{\text{ph}} = V_{\text{LO}} + V_{\text{ac}}$ and the total screened electron-phonon interaction $V_{\text{sc-ph}}$ can be separated into $V_{\text{sc-LO}}$ (as determined before) plus the screened electron interactions with acoustic phonons: $V_{\text{sc-ph}} = V_{\text{sc-LO}} + V_{\text{sc-ac}}$. Solving for $V_{\text{sc-ac}}$,

$$V_{\text{sc-ac}}(q,\omega) = \frac{V_{\text{LO}} + V_{\text{ac}}}{\epsilon[1-(v_q^\infty + V_{\text{LO}} + V_{\text{ac}})P]} - \frac{V_{\text{LO}}}{\epsilon[1-(v_q^\infty + V_{\text{LO}})P]} \tag{3}$$

$$= \frac{V_{\text{ac}}}{(\epsilon - V_{\text{LO}}P - V_{\text{ac}}P)(\epsilon - V_{\text{LO}}P)}\,. \tag{4}$$

Since the acoustic-phonon frequencies are small for relevant q values, $V_{\text{sc-ac}}$ is evaluated in the static limit. Using $V_{\text{LO}}(q,\omega=0) = v_q(\epsilon_0^{-1} - \epsilon_\infty^{-1})$, which implies that $\epsilon - V_{\text{LO}}P = 1 - v_qP/\epsilon_0$, we have

$$V_{\text{sc-ac}} = \frac{\epsilon_0^2 V_{\text{ac}}}{(\epsilon_0 - v_qP)^2[1-\epsilon_0 V_{\text{ac}}P/(\epsilon_0 - v_qP)]}\,. \tag{5}$$

Thus ϵ_0 appears in the acoustic mode screening function. The acoustic-phonon self-energy $\epsilon_0 V_{\text{ac}}P/(\epsilon_0 - v_qP)$ is neglected in the present work.

The electron-impurity interaction may also be viewed as a test-charge–test-charge interaction. Since the scattering process is assumed to be nearly elastic, the relevant

screening function is $\epsilon_T(q,\omega)$ evaluated at $\omega=0$. In this case, ϵ_T should include the electronic and LO-phonon parts plus a contribution from the piezoelectric phonon interaction. The piezoelectric contribution is assumed to be small and is neglected here so that the screening function for the electron-impurity interaction is $\epsilon_0 - v_q P$, the same as for the acoustic modes.

III. NUMERICAL METHOD

In order to solve the electron Boltzmann equation for a weak electric field $\mathbf{F}$, the nonequilibrium distribution function $f(\mathbf{k}_i)$ may be expanded around the equilibrium solution $f_i^0 = \{1-\exp[\beta(E_i-\mu)]\}^{-1}$ to first order in $\mathbf{F}$,

$$f(\mathbf{k}_i) = f_i^0 + f_i^0(1-f_i^0)x_i\psi_i\,, \tag{6}$$

where x_i is the cosine of the angle between $\mathbf{F}$ and $\mathbf{k}_i$ and $\psi_i = \psi(k_i)$ is a function that is linear in F, but is otherwise unknown and to be determined by solving the Boltzmann equation. Rode[1] devised and implemented an iterative procedure for solving the Boltzmann equation to determine $f(\mathbf{k})$ to first order in $\mathbf{F}$ for the case of spherical energy surfaces, including electron-phonon and electron-impurity scattering only. Assuming the linear form of f (6) and using the law of cosines in the electron Boltzmann equation [Eq. (39) of Ref. 20] gives an integral equation for the nonequilibrium electron distribution function[1]

$$\begin{aligned}\frac{eF}{\hbar}\frac{\partial f_k^0}{\partial k}x_k &= -\{\dot{f}_k\}_{\rm coll}^{\rm linear}\\ &= \frac{x_k}{\Omega}\sum_{\mathbf{p}} g_p x_{kp}\{W(\mathbf{k},\mathbf{p})[1-f_k^0] + W(\mathbf{k},\mathbf{p})f_k^0\}\\ &\quad -g_k\frac{x_k}{\Omega}\sum_{\mathbf{p}}\{W(\mathbf{k},\mathbf{p})[1-f_p^0] + W(\mathbf{p},\mathbf{k})f_p^0\},\end{aligned} \tag{7}$$

where $g_k = f_k^0(1-f_k^0)\psi_k$, x_{kp} is the cosine of the angle between $\mathbf{k}$ and $\mathbf{p}$, and $W(\mathbf{k},\mathbf{p})$ is the total differential scattering rate for electronic transitions from state $|\mathbf{k}\rangle$ to state $|\mathbf{p}\rangle$ due to scattering from ionized impurities and phonons.

In the present work, $W(\mathbf{k},\mathbf{p})$ for the interaction with LO phonons is modified to include the plasmon-phonon coupling as described in Ref. 20. Approximating the phonon distribution function by its equilibrium form $N^0(\omega) = (e^{\beta\hbar\omega}-1)^{-1}$ and using the plasmon-pole approximation on the phonon self-energy gives

$$\begin{aligned}W^{\rm LO}(\mathbf{k},\mathbf{p}) &= \frac{-2M_q^2}{\Omega\hbar|\epsilon(q,\omega_{k,p})|^2}[N^0(\omega_{k,p})+1]\\ &\quad\times{\rm Im}[D^+(q,\omega_{k,p}) + D^-(q,\omega_{k,p})],\end{aligned} \tag{8}$$

$$\begin{aligned}{\rm Im}[D^{\pm}(q,\omega)] &= \mp\frac{\pi\omega_{\rm TO}(\omega^2-\tilde{\omega}_p^2)}{\hbar\omega_{\pm}(\omega_+^2-\omega_-^2)}\\ &\quad\times[\delta(\omega+\omega_{\pm}) - \delta(\omega-\omega_{\pm})]\,,\end{aligned} \tag{9}$$

where $M_q^2 = v_q(\epsilon_\infty^{-1}-\epsilon_0^{-1})\hbar\omega_{\rm LO}^2/2\omega_{\rm TO}$ and the frequencies $\tilde{\omega}_p$, ω_+, and ω_- are given by

$$\tilde{\omega}_p^2 = \omega_p^2[1-\epsilon^{-1}(q,0)]^{-1}, \tag{10}$$

$$\omega_{\pm}^2 = \frac{1}{2}\Big\{\omega_{\rm LO}^2 + \tilde{\omega}_p^2 \pm \left[(\omega_{\rm LO}^2-\tilde{\omega}_p^2)^2 + 4\omega_p^2(\omega_{\rm LO}^2-\omega_{\rm TO}^2)\right]^{1/2}\Big\}. \tag{11}$$

The weight factors $(\omega_{\pm}^2-\tilde{\omega}_p^2)(\omega_+^2-\omega_-^2)^{-1}$ in ${\rm Im}[D^{\pm}]$ give the phonon strength in each of the hybrid $\omega_{\pm}$ modes, so that the differential scattering rate $W^{\rm LO}$ is the rate for scattering from only the phonon component of the hybrid modes. The screening function for the LO phonons is the electronic part of the total dielectric function $\epsilon(q,\omega) = 1 - v_q^\infty P(q,\omega)$.

Rode's iterative method can be generalized to include electron-electron scattering by adding the linearized version of the electron-electron collision term $\{\dot{f}\}_{\rm coll}^{e\text{-}e}$ [Eq. (46) of Ref. 20] to the right-hand side of (7) before solving for ψ_k. The Appendix shows how this is done by again using the law of cosines and simplifying $\{\dot{f}\}_{\rm coll}^{e\text{-}e}$. Then, the nonequilibrium function ψ satisfies the integral equation

$$\psi(k) = \left[\nu_{\rm inel}[\psi(k)] - \frac{eF}{\hbar}\frac{\partial f_k^0}{\partial k}\right] \times\left[\frac{1}{\tau_{e\text{-}e}(k)} + f_k^0(1-f_k^0)\left(\frac{1}{\tau_{\rm el}(k)} + \frac{1}{\tau_{\rm LO}(k)}\right)\right]^{-1}, \tag{12}$$

with the terms defined in this section.

For elastic scattering processes, the identities $k=p$ and $W(\mathbf{k},\mathbf{p}) = W(\mathbf{p},\mathbf{k})$ apply in Eq. (7) so that the elastic scattering rate has the form

$$\tau_{\rm el}^{-1}(k) = \frac{1}{\Omega}\sum_{\mathbf{p}}(1-x_{kp})\,W_{\rm el}(\mathbf{k},\mathbf{p})\,. \tag{13}$$

Interactions with acoustic phonons are approximated as elastic so that $\tau_{\rm el}^{-1}$ is composed of the rates for acoustic deformation potential, piezoelectric, and ionized impurity scattering, $\tau_{\rm el}^{-1}(k) = \tau_{\rm DP}^{-1}(k) + \tau_{\rm pe}^{-1}(k) + \tau_{ii}^{-1}(k)$. The acoustic mode scattering rates are calculated as in Ref. 1 except the interactions are screened in the static RPA as described in Sec. II,

$$\frac{1}{\tau_{\rm DP}(k)} = \frac{E_1^2 k_B T m^*}{4\pi\hbar^3 c_l k^3}\int_0^{2k} dq\frac{q^3}{[1-v_qP(q,0)/\epsilon_0]^2}, \tag{14}$$

$$\frac{1}{\tau_{\rm pe}(k)} = \frac{e^2P_{\rm pe}^2 k_B T m^*}{\epsilon_0\hbar^3 k^3}\int_0^{2k} dq\frac{q}{[1-v_qP(q,0)/\epsilon_0]^2}, \tag{15}$$

where E_1 is the acoustic deformation potential, c_l is the spherically averaged elastic constant for longitudinal modes, and $P_{\rm pe}$ is the piezoelectric coefficient.

The electron-impurity scattering rate $1/\tau_{ii}^{\rm PS}$ is calculated with the phase shifts $\delta_l(k)$ determined by numerically solving the radial Schrödinger equation with an

impurity potential screened with the static RPA total dielectric function $\epsilon_T(q,0)$.[14] The results presented below include a comparison with the Born approximation $1/\tau_{ii}^{\rm Born}$,

$$\frac{1}{\tau_{ii}^{\rm PS}(k)} = \frac{4\pi\hbar}{km^*}N_i\sum_{l=0}^{\infty}(l+1)\sin^2[\delta_l(k)-\delta_{l+1}(k)], \quad (16)$$

$$\frac{1}{\tau_{ii}^{\rm Born}(k)} = \frac{4\pi^4 m^*}{\epsilon_0^2(\hbar k)^3}N_i\int_0^{2k} dq\frac{1}{q}\frac{1}{[1-v_qP(q,0)/\epsilon_0]^2}, \quad (17)$$

where N_i is the ionized impurity concentration.

The LTFA is made by using the temperature-dependent Thomas-Fermi dielectric function $\epsilon_{\rm LTFA}=1+q_{\rm TF}^2/q^2$, where $q_{\rm TF}^2=4\pi e^2/\epsilon(\partial n/\partial\mu)$ and μ is the chemical potential. The dielectric constant ϵ is ϵ_∞ for electron-electron or electron–LO-phonon scattering, while $\epsilon=\epsilon_0$ for the screened impurity and the acoustic-phonon potentials. Using the LTFA in Eq. (17) gives the familiar Brooks-Herring formula.

The inverse lifetimes $\tau_{e\text{-}e}^{-1}(k)$ and $\tau_{\rm LO}^{-1}(k)$ describe the rate at which the nonequilibrium population of state $|\mathbf{k}\rangle$ decays due to inelastic scattering with the equilibrium population of the other states. For electron-electron collisions,

$$\tau_{e\text{-}e}^{-1}(k) = \frac{8e^4 f_k}{\epsilon_\infty^2\hbar k}\int_0^\infty dp\,p(1-f_p)[N^0(\omega_{k,p})+1] \times\int_{|k-p|}^{k+p}\frac{dq}{q^3}\frac{{\rm Im}[P(q,\omega_{k,p})]}{|\epsilon(q,\omega_{k,p})|^2}. \quad (18)$$

For scattering with the LO-phonon component of the hybrid modes,

$$\tau_{\rm LO}^{-1}(k) = \sum_{\lambda=\pm}\lambda\Bigg\{\int_{|k-k_\lambda^-|}^{k+k_\lambda^-}dqI(q,\omega_\lambda)\Big[N^0(\omega_\lambda)+1-f_{k_\lambda^-}^0\Big] \times\Theta(E_k-\hbar\omega_\lambda) + \int_{|k-k_\lambda^+|}^{k+k_\lambda^+}dqI(q,\omega_\lambda)\Big[N^0(\omega_\lambda)+f_{k_\lambda^+}^0\Big]\Bigg\}, \quad (19)$$

where

$$k_\lambda^\pm = \sqrt{k^2\pm 2m^*\omega_\lambda/\hbar},$$

$$I(q,\omega_\lambda) = \frac{e^2\omega_{\rm LO}m^*}{q\omega_\lambda\hbar^2 k}\left(\frac{1}{\epsilon_\infty}-\frac{1}{\epsilon_0}\right)|\epsilon(q,\omega_\lambda)|^{-2}\frac{(\omega_\lambda^2-\tilde\omega_p^2)}{(\omega_+^2-\omega_-^2)}.$$

Since the mobility is measured on a system with *all* of the electrons out of equilibrium, the linear integral equation (12) also contains the functional $\nu_{\rm inel}[\psi]$ describing the rate of change of the equilibrium occupation of the state $|\mathbf{k}\rangle$ due to inelastic scattering with the nonequilibrium population of the other states. This term is composed of electron-electron and electron–LO-phonon parts $\nu_{\rm inel}=\nu_{e\text{-}e}+\nu_{\rm LO}$. The contribution from electron-electron scattering is

$$\nu_{e\text{-}e}[\psi] = \frac{-4e^4 f_k^0}{\epsilon_\infty^2\hbar k^2}\int_0^\infty dp\,(1-f_p^0)\int_{|k-p|}^{k+p}\frac{dq}{q^3}|\epsilon(q,\omega_{k,p})|^{-2} \times\Bigg\{\psi_p(k^2+p^2-q^2)[N^0(\omega_{k,p})+1]{\rm Im}[P(q,\omega_{k,p})] + \frac{m^*p}{2\pi\hbar^2q^2}(k^2-p^2+q^2)\left[z^-\int_{|z^-|}^\infty ds\,\psi_s f_s^0(1-f_{s^+}^0) - z^+\int_{|z^+|}^\infty ds\,\psi_s f_{s^-}^0(1-f_s^0)\right]\Bigg\}, \quad (20)$$

where $z^\pm=(k^2-p^2\pm q^2)/2q$ and $s^\pm=\sqrt{s^2\pm(k^2-p^2)}$. The contribution from the LO-phonon strength in the hybrid modes is

$$\nu_{\rm LO}[\psi] = \sum_{\lambda=\pm}\lambda\Bigg\{\int_{|k-k_\lambda^-|}^{k+k_\lambda^-}dqI(q,\omega_\lambda)g(k_\lambda^-)\frac{[k^2+(k_\lambda^-)^2-q^2]}{2kk_\lambda^-}\left[N^0(\omega_\lambda)+f_k^0\right]\Theta(E_k-\hbar\omega_\lambda) + \int_{|k-k_\lambda^+|}^{k+k_\lambda^+}dqI(q,\omega_\lambda)g(k_\lambda^+)\frac{[k^2+(k_\lambda^+)^2-q^2]}{2kk_\lambda^+}[N^0(\omega_\lambda)+1-f_k^0]\Bigg\}. \quad (21)$$

Plasmon-phonon coupling may be neglected by setting ω_+ equal to $\omega_{\rm LO}$ and ω_- equal to $\tilde\omega_p$ in Eqs. (19) and (21).

IV. RESULTS AND DISCUSSION

The numerical results for the drift mobility were obtained by solving the iterative equation (12) with (6) for the linearized nonequilibrium electron distribution in order to determine the average velocity per unit electric field. The effective electron mass value $m^*=0.07m_e$ was used throughout the calculations. The other material parameters used were taken from Ref. 25. Results for uncompensated n-type GaAs are presented for conventionally doped material (Figs. 1–4) and for a doped system with no impurities present, an idealized model of modulation doped material (Figs. 5–7).

A. RPA vs LTFA screening

The LTFA is an approximation to the static RPA dielectric function that does not account for the polarization of the screening electrons by the colliding electron, but is equivalent in the limit of small momentum transfer, q. Figures 1 and 2 show the carrier concentration dependence of electron mobility in uncompensated n-type GaAs at 300 and 77 K, calculated with statically screened electron-phonon and electron-impurity interactions. Scattering from LO phonons as well as the acoustic piezoelectric and deformation potential modes was included, but electron-electron scattering and plasmon-phonon coupling were neglected. Each figure shows calculations made by using either the phase-shift (16) or the Born (17) electron-impurity scattering rate and either the temperature-dependent static RPA or the LTFA dielectric function in Eqs. (14)–(17). The standard LTFA Born (Brooks-Herring) calculation with unscreened phonons is also shown. Compared to the case of n-type Si,[14] a relatively small correction to mobility in n-type GaAs is obtained by using RPA screening rather than LTFA. Except for the unscreened phonon case at 300 K, the combination of RPA screening of impurities and phonons with the phase-shift electon-impurity scattering rate gives the lowest mobilities, while the LTFA Born calculations give values that are higher by at most 16% at 300 K and 41% at 77 K. A cancellation of errors made by using the LTFA Born electron-impurity interaction and unscreened electron-phonon interactions at 300 K makes this result similar in magnitude to the RPA Born curve. Dynamic RPA screening of LO phonons changes the mobility very little from the static RPA case when electron-impurity scattering is included.

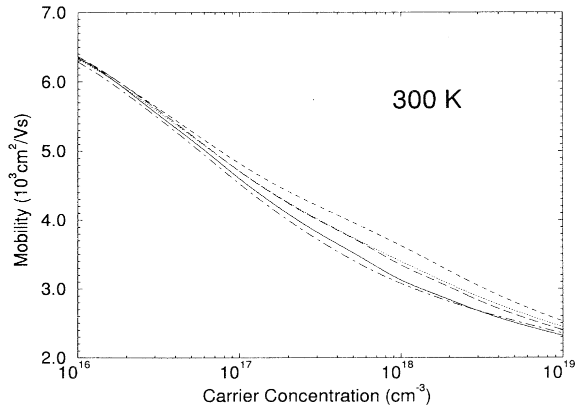

FIG. 1. Comparison of RPA vs LTFA screening and phase-shift vs Born electron-impurity cross sections at 300 K for n-type GaAs. Static screening of LO, piezoelectric, and acoustic deformation potential phonons as well as ionized impurities is included. The RPA phase-shift drift mobility (solid curve) is shown with mobilities in the following approximations: RPA Born (dotted curve), LTFA phase-shift (long-dashed curve), LTFA Born (short-dashed curve), and LTFA Born with unscreened phonons (chain-dashed curve). Electron-electron scattering and plasmon-phonon mode coupling has been neglected.

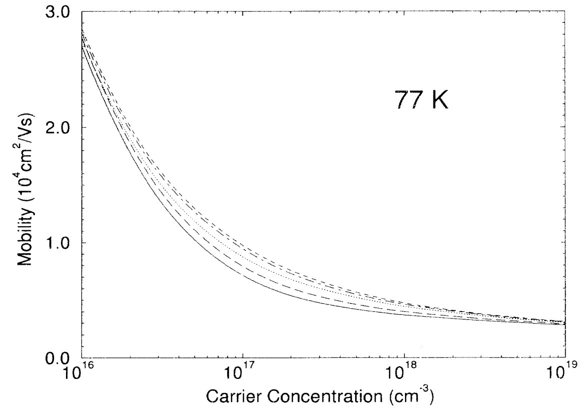

FIG. 2. Comparison of RPA vs LTFA screening and phase-shift vs Born electron-impurity cross sections at 77 K for n-type GaAs. Calculated mobilities are represented as in Fig. 1.

B. Electron-electron scattering

The effect of electron-electron scattering on mobility in doped semiconductors is limited by three factors. (i) The screened interaction between two electrons is considerably weaker than the Coulomb interaction. (ii) When umklapp electronic scattering processes are negligible and energy surfaces are close to spherical, electron-electon scattering conserves total electron momentum and produces only an indirect effect on other scattering processes by redistributing the electron momenta. (iii) The Pauli principle restricts the fraction of electrons that can participate in energy-conserving electron-electron scattering processes to a number that vanishes in the degenerate limit. Nevertheless, electron-electron scattering was shown[26] to have an important effect on transport in doped semiconductors away from the degenerate limit. Chattopadhyay[8] studied its effect on mobility in n-type GaAs by using a variational solution of the Boltzmann equation including electron-electron scattering statically screened in LTFA with ϵ_0. He found that, for $n = 10^{16}$ cm^{-3}, electron-electron scattering reduces the mobility by about 10% at 80 K. The reduction increases to 20% when ϵ_∞ rather than ϵ_0 is used in the LTFA screened electron-electron interaction, as discussed in Ref. 20. Figures 3 and 4 show the drift mobility calculated by iteratively solving the Boltzmann equation at 300 and 77 K, including electron-electron scattering in addition to the electron-impurity and electron-phonon mechanisms already discussed. The Pauli principle restriction is clearly seen from the vanishing of the electron-electron contribution at higher concentrations. Also shown in Figs. 3 and 4 are experimental data[6,9,27] for the Hall mobility of n-type GaAs. No attempt has been made in the calculations to include the Hall factor relating the drift to Hall mobilities. The Hall factor is generally larger than unity so that the Hall mobility is larger than the drift mobility, but its magnitude depends on doping density and temperature, approaching unity in the degenerate limit. Despite the reduced mobility values

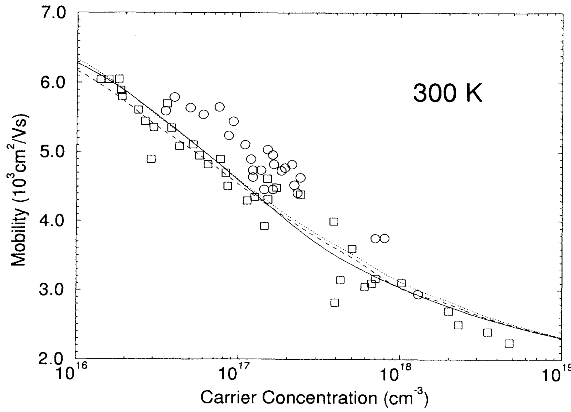

FIG. 3. Effect of electron-electron scattering on electron drift mobility in n-type GaAs at 300 K. The dotted and dashed curves are the RPA phase-shift calculation neglecting and including, respectively, statically screened electron-electron scattering. The solid curve includes dynamically screened electron-electron and electron–LO-phonon scattering with mode coupling. Experimental Hall mobilities are indicated by ○ (Ref. [9]) and □ (Ref. 27).

compared to previous calculations (see, e.g., Refs. 1, 2, 4, and 7), a disagreement between theory and experiment persists for carrier concentrations above $n = 10^{18}$ cm^{-3} at both temperatures considered.

C. Coupled plasmon-phonon modes

The uncoupled plasmon temperature $\hbar\omega_p/k_B$ varies as $n^{1/2}$; for n-type GaAs, it ranges from 50 K to 1594 K for electron concentrations of 10^{16}–10^{19} cm^{-3}. The plasmon temperature crosses the LO-phonon temperature of 419 K at $\sim 7 \times 10^{17}$ cm^{-3}. In this concentration region, the electronic and the lattice excitations hybridize to form the normal modes of mixed electron-phonon character. The other energy relevant to electron mobility is the Fermi energy E_F, which varies as $n^{2/3}$. For n-type GaAs, E_F/k_B ranges from 29 K to 2930 K for $n = 10^{16}$–10^{19} cm^{-3} and crosses the LO-phonon temperature at $\sim 6 \times 10^{17}$ cm^{-3}.

In the plasmon-pole model, the phonon spectral function $-\pi^{-1}\text{Im}[D(q,\omega)]$ has two δ-function peaks [see Eq. (9)] with frequencies ω_+ and ω_- given by (11). As discussed in Ref. 20, mobilities at low densities and temperatures are expected to be reduced when plasmon–LO-phonon coupling is included, because of increased low-energy electron-phonon scattering due to the ω_- mode. Figure 5 shows that this is in fact the case. The mobilities in this figure were calculated by neglecting all scattering mechanisms except electron–LO-phonon scattering. For a wide range of densities at 77 K, the LO-phonon limited mobility including mode coupling and dynamic RPA screening (solid curve) is significantly lower than the mobilites calculated by neglecting these effects. The dip observed below $n = 10^{18}$ cm^{-3} in all the Fig. 5 mobility curves is related to E_F crossing the LO-phonon emission threshold. An interesting though minor effect appears in Fig. 3, where the mobility including mode coupling is actually higher at low doping levels and 300 K than the mobility neglecting the coupling, when electron-impurity is included.

Since mobility is limited primarily by scattering from ionized impurities at low temperatures in conventionally doped GaAs, the mode-coupling effect is obscured in this case. Nevertheless, it could be important for mobility in modulation doped structures where the effects of impurity scattering are greatly reduced because of the large separation between dopants and carriers. Figure 6 plots the electron drift mobility as a function of concentration at 77 K when electron-impurity scattering is neglected. The figure shows that scattering from the acoustic (piezoelectric and deformation potential) modes is stronger

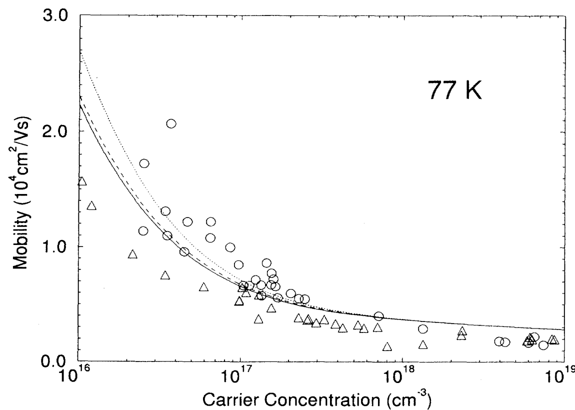

FIG. 4. Effect of electron-electron scattering on electron drift mobility in n-type GaAs at 77 K. Calculated mobilities are represented as in Fig. 3. Experimental Hall mobilities are indicated by ○ (Ref. 9) and △ (Ref. 12).

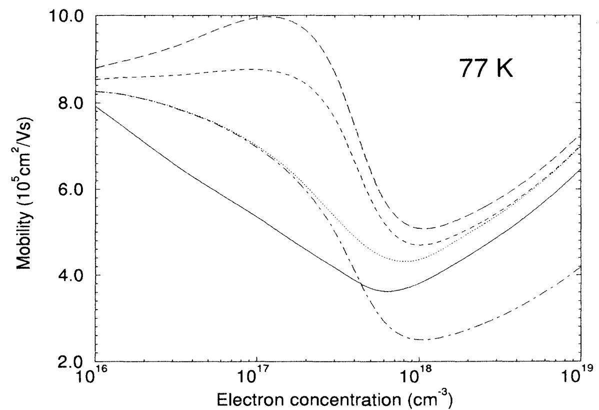

FIG. 5. Effects of screening and mode coupling on LO-phonon limited electron mobility in n-type GaAs at 77 K. The dynamically screened coupled mode mobility calculation (solid curve) is compared to mobilities determined by scattering from uncoupled LO phonons screened with LTFA (long-dashed curve), static RPA (short-dashed curve), dynamic RPA (dotted curve), and unscreened (chain-dashed curve). All other scattering mechanisms are neglected.

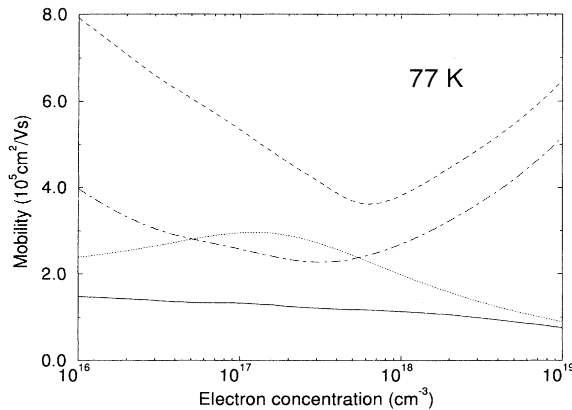

FIG. 6. Comparison of mobilities limited by inelastic and acoustic-phonon scattering in n-type GaAs at 77 K. The mobility including dynamically screened electron-electron and electron–LO-phonon scattering including mode coupling (long-dash–short-dashed curve) is compared to the same calculation except neglecting electron-electron scattering (dashed curve) and to the mobility including only scattering from acoustic (piezoelectric and deformation potential) phonons screened with static RPA (dotted curve). The solid curve shows the calculated mobility including all of the mechanisms. Electron-impurity scattering is not included.

than scattering from LO phonons when electron-electron scattering is neglected, even if mode coupling is included. However, in the moderate doping regime, inelastic scattering is stronger than scattering from acoustic phonons when both electron-electron scattering and mode coupling are included. This result is notable especially because the value used in the calculation for the acoustic deformational potential $E_1 = 12$ eV is higher than some others that appear in the literature. Figure 7 plots the temperature dependence of the mobility from 50 to 150 K for $n = 10^{17}$ cm^{-3} when electron-impurity scattering is neglected. The figure shows that electron-electron scattering and mode-coupling effects should be significant even at the lower temperatures in situations where impurity effects are minimal.

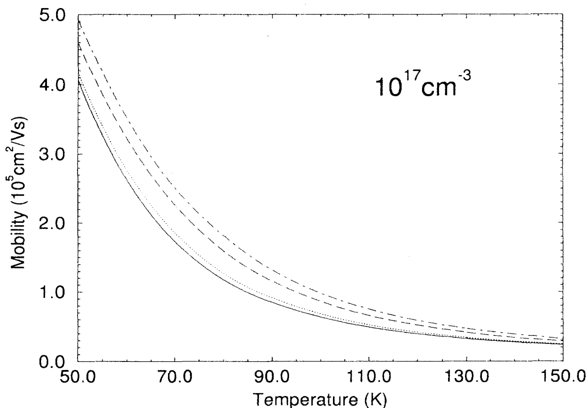

FIG. 7. Temperature dependence of mobility in n-type GaAs for $n = 10^{17}$ cm^{-3}. The mobility including dynamically screened electron-electron and electron–LO-phonon scattering including mode coupling (solid curve) is compared to the results with static RPA screening of electron-electron scattering (dotted curve), electron-electron scattering neglected (dashed curve), and static RPA screening of LO phonons without mode coupling (long-dash–short-dashed curve). Electron scattering from acoustic phonons screened in static RPA is included and electron-impurity scattering is neglected in all cases.

V. CONCLUSIONS

The mobility calculations presented in this paper show that a more accurate treatment of electron interactions in n-type GaAs yields results that differ from simple models, especially at moderate doping levels in conventionally doped material and for low densities and temperatures in modulation-doped material. For conventional n-type GaAs, RPA screening of phonons and impurities combined with phase-shift electron-impurity scattering rates give lower drift mobilities than LTFA screening or Born calculations. A convergent iterative method has been developed for solving the Boltzmann equation including electron-electron scattering. Including this scattering mechanism further reduces the mobility except at high doping levels, so that the full calculation gives better agreement with experimental Hall mobilities than previous results. In order to say definitively that the long-standing discrepancy between theory and experiment is resolved in the middle concentration regime, the Hall mobility should be calculated with the present model, including the influence of nonequilibrium phonons. At the highest concentrations, the theoretical mobility for uncompensated n-type GaAs is larger than experimental values.

The effects of dynamic screening, mode coupling, and electron-electron scattering are not very important for mobility in conventionally doped GaAs where scattering from ionized impurities dominates. However, the calculations neglecting impurities suggest that these effects could significantly affect mobilities in modulation-doped structures. Comparison with experiment would require a more realistic treatment including the effects of confinement on phonon spectra and electronic structure, nonequilibrium phonons, as well as the effects of impurities, alloy disorder, and interface roughness. Also, the effect of Landau damping of the hybrid modes, which is neglected in the plasmon-pole model for the phonon self-energy, should be investigated. Good candidates for study would be $Al_xGa_{1-x}As$, since the Fröhlich coupling increases with x,[28] or the more strongly polar materials CdTe, ZnSe, or ZnTe. Finally, the fact that inelastic scattering is stronger compared to acoustic-phonon scattering than the standard model predicts for doped material at low temperature suggests that the inelastic component could influence determinations of the deformation potential constant from mobility studies and motivates a reevaluation of E_1 in n-type GaAs at low temperatures.

ACKNOWLEDGMENTS

I thank J.R. Lowney, G.W. Bryant, S. Das Sarma, and P.B. Allen for helpful conversations.

APPENDIX: ITERATIVE METHOD FOR ELECTRON-ELECTRON SCATTERING

Rode's method[1] is generalized by inserting the linearized form of f (6) into the electron-electron collision term [Eq. (46) of Ref. 20] and using the identity

$$\delta(E_1+E_2-E_3-E_4) \times\left[f_1^0 f_2^0(1-f_3^0)(1-f_4^0)-(1-f_1^0)(1-f_2^0)f_3^0 f_4^0\right]=0, \tag{A1}$$

giving the linearized collision term

$$\{f(\mathbf{k}_1)\}_{\text{coll}}^{e\text{-}e}=\frac{1}{\Omega^3}\sum_{2,3,4}|M_{3,1}|^2\delta(E_1+E_2-E_3-E_4) \times\delta(\mathbf{k}_1+\mathbf{k}_2-\mathbf{k}_3-\mathbf{k}_4) \times f_1^0 f_2^0(1-f_3^0)(1-f_4^0) \times[x_1\psi_1+x_2\psi_2-x_3\psi_3-x_4\psi_4]\,.$$

This symmetric form allows a simple application of the law of cosines to eliminate x_i for $i=2$–4 in favor of x_{1i}, the cosine of the angle between $\mathbf{k}_1$ and $\mathbf{k}_i$,

$$\{f(\mathbf{k}_1)\}_{\text{coll}}^{e\text{-}e}=\frac{x_1}{\Omega^3}\sum_{2,3,4}|M_{3,1}|^2\delta(E_1+E_2-E_3-E_4) \times\delta(\mathbf{k}_1+\mathbf{k}_2-\mathbf{k}_3-\mathbf{k}_4) \times f_1^0 f_2^0(1-f_3^0)(1-f_4^0) \times[\psi_1+x_{12}\psi_2-x_{13}\psi_3-x_{14}\psi_4]\,. \tag{A2}$$

Now use the δ function for momentum conservation to sum over $\mathbf{k}_4$ and introduce the variable $\mathbf{q}=\mathbf{k}_1-\mathbf{k}_3=\mathbf{k}_4-\mathbf{k}_2$. The $\mathbf{k}_2$ integration of the ψ_1 and ψ_3 terms can be done analytically. Making the variable changes $\mathbf{k}_1\to\mathbf{k}, \mathbf{k}_2\to\mathbf{s}, \mathbf{k}_3\to\mathbf{p}=\mathbf{k}-\mathbf{q}$, and $\mathbf{k}_4\to\mathbf{s}+\mathbf{q}$, we have

$$\begin{aligned}\{f(\mathbf{k})\}_{\text{coll}}^{e\text{-}e}=&\frac{-x_k}{2\pi\Omega}\sum_{\mathbf{p}}|M_{k,p}|^2(\psi_k-x_{kp}\psi_p)[N^0(\omega_{k,p})+1]\text{Im}[P(q,\omega_{k,p})]f_k^0(1-f_p^0)\\ &+\frac{1}{\Omega^2}\sum_{\mathbf{s},\mathbf{p}}|M_{k,p}|^2 x_{ks}\,\psi_s\{\delta(E_k-E_p+\hbar\omega_{s,s+q})f_k^0 f_s^0(1-f_p^0)(1-f_{s+q}^0)\\ &-\delta(E_k-E_p-\hbar\omega_{s,s-q})f_k^0 f_{s-q}^0(1-f_p^0)(1-f_s^0)\}\,,\end{aligned} \tag{A3}$$

where $\mathbf{s}$ was changed to $\mathbf{s}-\mathbf{q}$ in the last term and

$$\text{Im}[P(q,\omega)]=\frac{m^*}{2\pi\hbar^4\beta q}\ln\left|\frac{1+\exp[-\beta(E^+-\mu)]}{1+\exp[-\beta(E^--\mu)]}\right|\,, \tag{A4}$$

with $E^\pm=(E_q\pm\hbar\omega)^2/4E_q$.

The symmetry of the problem is best used by choosing bipolar coordinates[24] with the z axis along $\mathbf{q}$ and the xz plane containing $\mathbf{k}$. The $\mathbf{p}$ integration variables can be chosen to include the momentum transfer q,

$$\int d^3p=2\pi\int_0^\infty dp\,p\int_{|k-p|}^{k+p}dq\,\frac{q}{k}\,,$$

the factor of 2π coming from integration of the azimuthal angle around $\mathbf{k}$. The $\mathbf{s}$ integration has the form $\int d^3s=\int d\phi\int dx_{sq}\int ds\,s^2$, where ϕ is the angle between the $(\mathbf{k},-\mathbf{p})$ and $(-\mathbf{s},\mathbf{k}_4)$ plane. The ϕ integral is simply done by again applying the law of cosines,

$$\int_0^{2\pi}d\phi\,x_{ks}=2\pi\,x_{sq}\,x_{kq}\,.$$

Then, using the energy δ functions to do the x_{sq} integrals, the linearized electron-electron collision integral reduces to

$$\begin{aligned}\{f(\mathbf{k})\}_{\text{coll}}^{e\text{-}e}=&\frac{-x_k f_k^0}{k(2\pi)^3}\int_0^\infty dp\,p(1-f_p^0)\int_{|k-p|}^{k+p}dq|M_{k,p}|^2\\ &\times\Bigg\{q(\psi_k-x_{kp}\psi_p)[N^0(\omega_{k,p})+1]\text{Im}[P(q,\omega_{k,p})]\\ &+\frac{x_{kq}\,m^*}{2\pi\hbar^2}\left[z^-\int_{|z^-|}^\infty ds\,\psi_s f_s^0(1-f_{s^+}^0)-z^+\int_{|z^+|}^\infty ds\,\psi_s f_{s^-}^0(1-f_s^0)\right]\Bigg\}\,,\end{aligned} \tag{A5}$$

where $z^\pm=(k^2-p^2\pm q^2)/2q$ and $s^\pm=\sqrt{s^2\pm(k^2-p^2)}$. Adding (A5) to the right-hand side of (7) and solving for ψ_k gives Eq. (12).

[1] D.L. Rode, in *Semiconductors and Semimetals*, edited by R.K. Willardson and A.C. Beer (Academic, New York, 1975), Vol. 10, Chap. 1.
[2] J.R. Lowney and H.S. Bennett, J. Appl. Phys. **69**, 7102 (1991).
[3] J.R. Meyer and F.J. Bartoli, Phys. Rev. B **36**, 5989 (1987).
[4] D. Lancefield, A.R. Adams, and M.A. Fisher, J. Appl. Phys. **62**, 2342 (1987).
[5] T.F. Kuech, B.S. Meyerson, and E. Veuhoff, Appl. Phys. Lett. **44**, 986 (1984).
[6] M. Feng, V.K. Eu, T. Zielinski, and J.M. Whelan, J. Electron. Mater. **11**, 663 (1982).
[7] W. Walukiewicz, L. Lagowski, L. Jastrzebski, M. Lichtensteiger, and H.C. Gatos, J. Appl. Phys. **50**, 899 (1979); W. Walukiewicz, J. Lagowski, and H.C. Gatos, *ibid.* **53**, 769 (1982).
[8] D. Chattopadhyay, J. Appl. Phys. **53**, 3330 (1982).
[9] G.B. Stringfellow, J. Appl. Phys. **50**, 4178 (1979).
[10] I.Y. Yanchev, B.G. Arnaudov, and S.K. Evtimova, J. Phys. C **12**, L765 (1979).
[11] H. Poth, H. Bruch, M. Heyen, and P. Balk, J. Appl. Phys. **49**, 285 (1978).
[12] D.L. Rode and S. Knight, Phys. Rev. B **3**, 2534 (1971); D.L. Rode, *ibid.* **2**, 1012 (1970).
[13] E.J. Moore, Phys. Rev. **160**, 618 (1967).
[14] B.A. Sanborn, P.B. Allen, and G.D. Mahan, Phys. Rev B **46**, 15 123 (1992).
[15] P. Lugli and D.K. Ferry, Physica **129B**, 532 (1985).
[16] M.E. Kim, A. Das, and S.D. Senturia, Phys. Rev. B **18**, 6890 (1978).
[17] R. Jalabert and S. Das Sarma, Phys. Rev. B **41**, 3651 (1990).
[18] S. Das Sarma, J.K. Jain, and R. Jalabert, Phys. Rev. B **41**, 3561 (1990).
[19] X.L. Lei and M.W. Wu, Phys. Rev. B **47**, 13 338 (1993).
[20] B.A. Sanborn, preceding paper, Phys. Rev. B **51**, 14 247 (1995).
[21] A.W. Overhauser, Phys. Rev. B **3**, 1888 (1971); B.I. Lundqvist, Phys. Kondens. Mater. **6**, 193 (1967); **6**, 206 (1967).
[22] S. Das Sarma, J.K. Jain, and R. Jalabert, Phys. Rev. B **37**, 4560 (1988); **37**, 6290 (1988).
[23] G.D. Mahan, *Many Particle Physics* (Plenum, New York, 1990), Sec. 6.3.
[24] M. Combescot and R. Combescot, Phys. Rev. B **35**, 7986 (1987).
[25] B.R. Nag, *Electron Transport in Compound Semiconductors* (Springer-Verlag, Berlin, 1980), p. 372.
[26] J. Appel, Phys. Rev. **125**, 1815 (1962); **122**, 1760 (1961).
[27] Y.-M. Houng and T.S. Low, J. Cryst. Growth **77**, 272 (1986).
[28] S. Adachi, J. Appl. Phys. **58**, R1 (1985).